http://mountain-risks.eu

Mountain Risks: 2007-2010

A Marie Curie Research & Training Network

MARIE CURIE ACTIONS

PREDICTION OF LANDSLIDES CRISES: TESTING CONCEPTS FOR FLUIDIZATION OF SLIDING MATERIAL

Th.W.J. van Asch [(1)], J.-P. Malet [(2)], B. Aksoy [(3)], B. van Dam [(1)], L.P.H. van Beek [(1)] & T.A. Bogaard [(1)]

(2) Faculty of Geosciences, Utrecht University, Utrecht, Netherlands.
(3) CNRS UMR 6554, University of Caen-Basse-Normandie, Caen, France.
(4) Polytech Grenoble, University Joseph Fourier, Grenoble, France.

Polytech'Grenoble

Contact:
Th.W.J. van Asch
Faculty of Geosciences, Utrecht University, Netherlands
Email: t.vanasch@geo.uu.nl

INTRODUCTION

Predicting the occurrence of landslide crises (eg. acceleration of gradually or intermittently moving landslides) is of paramount importance for a reliable assessment of the hazard. The main problem is to identify the possibilities of landslide acceleration and its potential transformation in a catastrophic flow. Different mechanisms has been identified which explain this dangerous transition.

- van Asch et al. (2006) proposed a conceptual mechanism describing fluidization by undrained loading caused by kinematic deformation of sliding material.
- Iverson (2005) proposed a mathematical model describing excess pore pressure generation and dissipation by dilation or contraction of the water saturated basal shear zone which is controlled by a dilatancy angle ψ, the hydraulic conductivity and the coefficient of consolidation of the material. This pore pressure generation controls the displacement rate during failure and may in case of positive excess pore pressure cause fluidization of the sliding material.

OBJECTIVE

The objective of this work is to present an experiment of retrogressively slumping in sandy silt material simulated in a laboratory flume. The laboratory simulations enable us to test whether liquefaction, which was observed in the flume can be explained by contraction of a saturated shear band or (and) by internal deformation and undrained loading.

LABORATORY EXPERIMENTS

The slumps were triggered by creating a critical steady state groundwater table by means of supply of a bottom head in the artificially slope and controlled drainage at the toe. Displacement rates could be determined through video monitoring (Fig. 1).

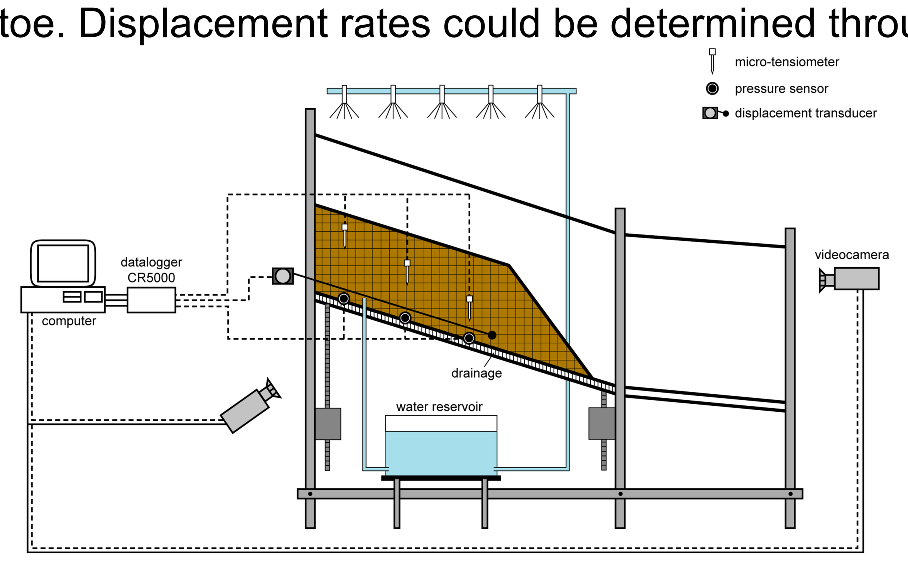

Fig. 1: A schematic picture of the laboratory flume.

A number of retrogressive slumps were observed in several experiments, which developed during a time span of about 1.5h. The slumps showed liquefaction during failure (Fig. 2)

The movement of the slumps were studied in detail by extracting image files from the video recorder. The geometry of each image was then registered with a image analysis software.

From the referenced images through time, 3 clearly visible "points" (A, B & C in Fig. 3) were tracked and their coordinates calculated to obtain displacements, and velocities (Fig. 4).

MODEL DESCRIPTION

Van Asch et al. (2006) assume that excess pore pressure is generated by compression or extension due to differences in velocity of the slices in a landslide.

The displacement T_i of the slice i and the velocity v_i is calculated assuming the generalized Bingham Coulomb-viscous model. The initial excess shear force for each slice is derived from the Bishop equations. It is assumed that, during the differential movement of the slices with a horizontal width b_i, and slip angle α_i, the most important dominant strain component (ε_{xx}) in the horizontal direction, can be calculated with (Eq. 1) :

$$\varepsilon_{xx} = -\frac{\left(\Delta T_{i+1}\cos\alpha_{i+1} - \Delta T\cos\alpha_i\right) + \left(\Delta T\cos\alpha_i - \Delta T_{i-1}\cos\alpha_{i-1}\right)}{b_i} \quad (1)$$

Fig. 2: Flume experiment; of retrogressive slumping and liquefaction.

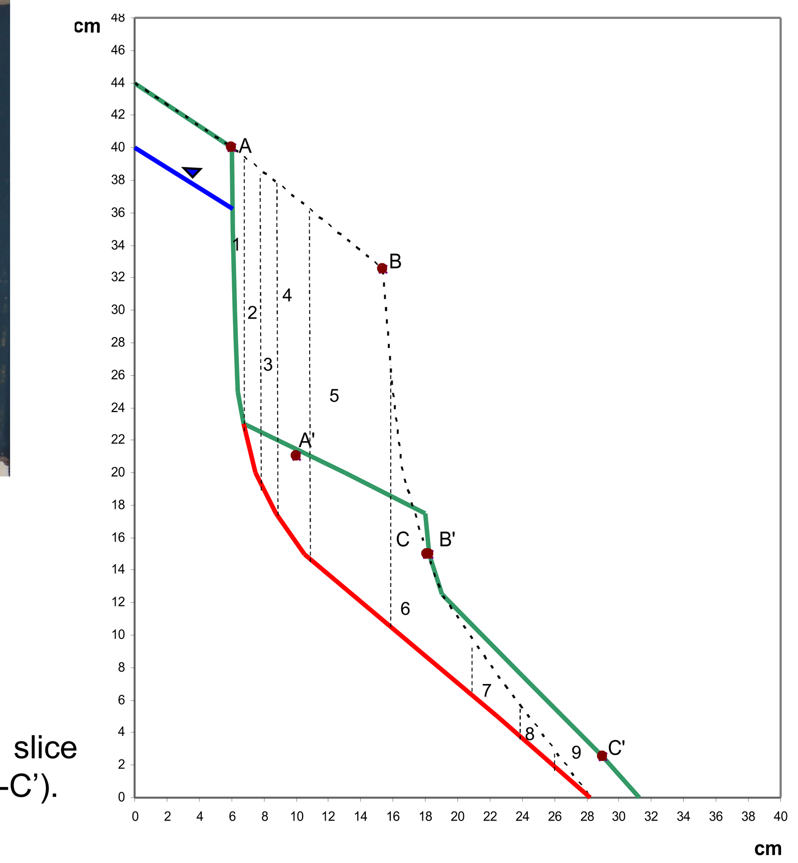

Fig. 3: The initial and final slump profile, the slice numbers and 3 displacement vectors (A-A', B-B', C-C').

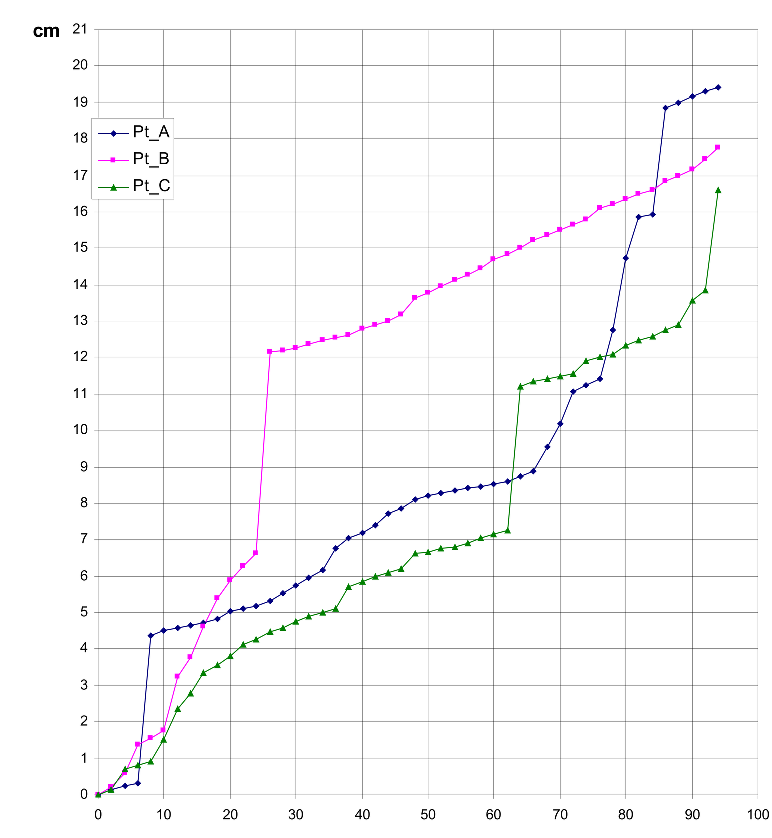

Fig. 4: Displacements in time of the points A, B & C.

$$\frac{\delta p_e}{\delta z} = \frac{\gamma_w g}{K}\psi v \quad (3)$$

where $\delta p_e/\delta z$ is the excess pore pressure gradient in the shear zone, γ_w is the bulk unit weight of water, g is the gravity acceleration, K_s is the hydraulic conductivity, ψ is the dilatancy angle ($\psi=\delta y/\delta x$ with respectively the displacement normal and parallel to the slip surface) and v is the displacement velocity along the slip surface.

Excess pore pressure Δu can be calculated with the Skempton's law (Eq. 2):

$$\Delta u = (1+A)\Delta\sigma_x = (1+A)\varepsilon_{xx}E \quad (2)$$

where A is Skempton's pore pressure coefficient and E the Young's modulus. The dissipation of excess pore pressure is obtained by calculating the degree of consolidation for uniform distribution of excess pore pressure in a half closed layer.

Iverson (2005) assumes that excess pore pressure is generated by dilation or compaction of the shear zone of a sliding block.

Iverson (2005) calculated the excess pore pressure in the shear zone which may dilate or compact during movement. The generated excess pore pressure gradient in the shear zone is calculated with (Eq. 3).

Drainage of excess pore pressure is obtained by computing the degree of consolidation for excess pore pressure, decreasing linearly with depth for an half closed layer.

MATERIAL PROPERTIES

The following geomechanical values, derived from triaxial tests, were selected for a loosely packed silty sand material (Fig.5).

Parameter	Symbol	Unit	Value
Skempton's pore pressure coefficient	A	(-)	0.5
Soil cohesion	c	kPa	0.5
Coefficient of consolidation	C_v	$m\ s^{-2}$	$1 \times 1\ 0^{-3}$
Young's elastic modulus	E	kPa	3.2×10^{3}
Hydraulic conductivity	K_s	$m\ s^{-1}$	2×10^{-4}
Soil friction angle	ϕ	(^{0})	36
Bulk unit weight of soil	γ_s	$kN\ m^{-3}$	16.9
Bulk unit weight of water	γ_w	$kN\ m^{-3}$	10
Apparent dynamic viscosity	η	K Pa s	8×10^{5}
Compaction angle	ψ	(^{0})	-6

Fig. 5: Geomechanical parameters used for the modeling exercise.

MODELLING RESULTS

The compression model shows for the parameters given in Fig. 5, after a displacement of 1.6 mm during 30 seconds, and liquefaction of slices n° 5, 6 & 7 (Fig. 3, Fig. 6). Due to the sharp curvature of the slip plane, liquefaction will always occur after a small displacement for a range of parametric values (C_v ,E, K_s) applicable for silty sand.

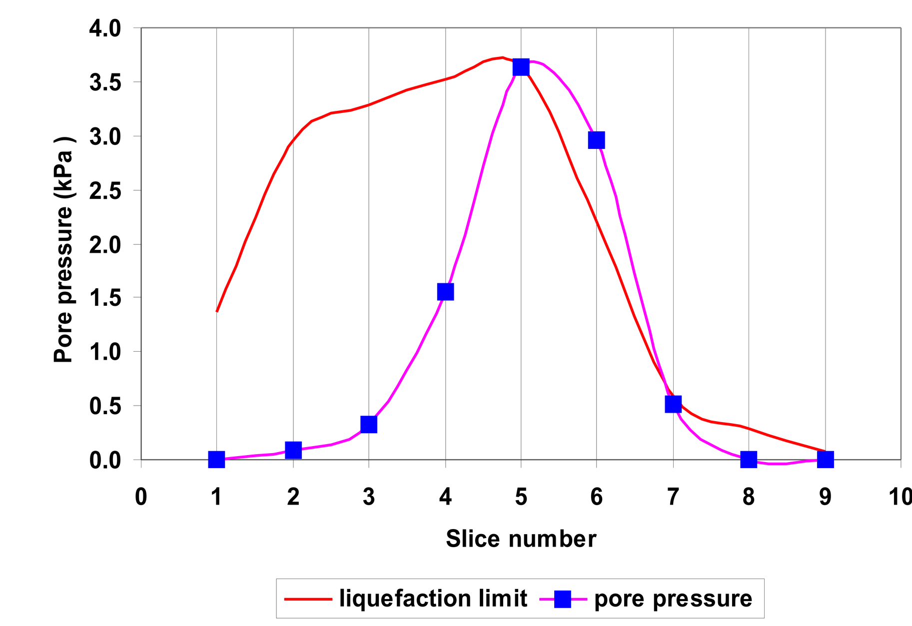

Fig. 6: Pore pressure distribution after 1.6 mm of displacement obtained by the kinematic compression model.

Figure 7 shows the results of the kinematic compaction model. In this case, a block sliding on the lower straight part of the slip surface with a height of 20 cm (Fig. 3) is assumed. The pore pressure reaches the liquid limit after a displacement of 20 cm (maximum displacement measured; see Fig. 4). Figure 7 also shows the theoretical development in case movement continues on an infinite slope. The compaction angle reduces to zero (no generation of excess pore pressure anymore), while excess pore pressure (p_e) dissipates and the total pore pressure decreases to its initial value p_i.

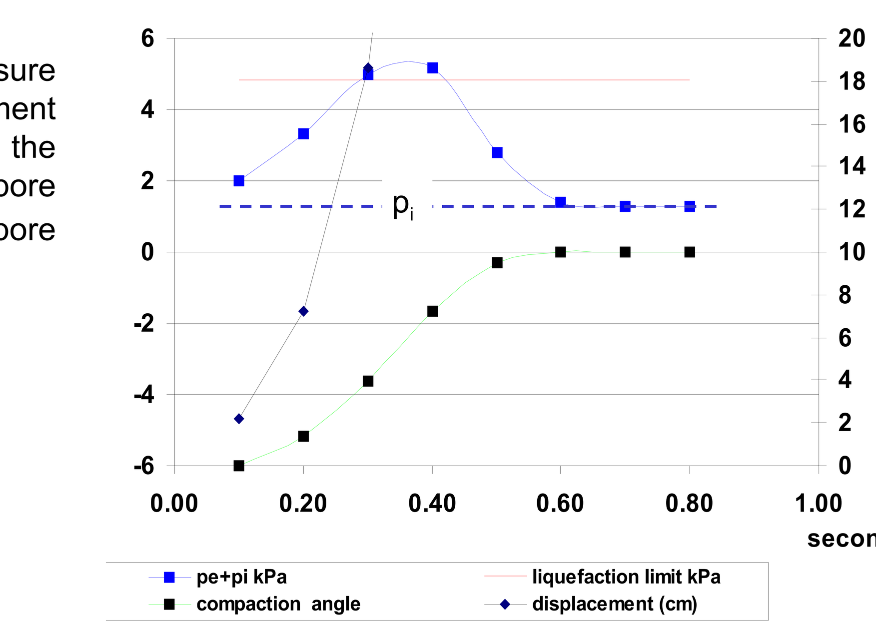

Fig. 7: Pore pressure development during displacement of a sliding block obtained with the compaction model (p_i is initial pore pressure, p_e is excess pore pressure)

CONCLUSIONS

Both models predict liquefaction of the slump. The kinematic compaction model always predicts liquefaction. The measured displacement rate is however 35 times higher than the calculated displacement. The compaction model shows liquefaction for K_s and ψ-values given in Fig. 5. There is no liquefaction when K_s increases and (or) ψ decreases. Displacements rates are however much higher (Fig. 6) than the measured rates (Fig. 4).

References:

Iverson, R.M., 2005. Regulation of landslide motion by dilatancy and pore pressure feedback. *Journal of Geophysical Research*: 110 F02015, doi.10.1029. 16 pp.

Van Asch, Th.W.J., Malet, J.-P., Van Beek, L.P.H., 2006. Influence of landslide geometry and kinematic deformation to describe the liquefaction of landslides: Some theoretical considerations. *Engineering Geology*: 88, pp. 59-69